Journal of Korean Association of Crystal Growth
Vol. 9, No. 2 (1999) 157-161

Estimation of mechanical damage by minority carrier recombination lifetime and near surface micro defect in silicon wafer

Chi-Young Choi and Sang-Hee Cho

Department of Inorganic Materials Engineering, Kyungpook National University, Taegu 702-701, Korea
(Received March 10, 1999)

실리콘 웨이퍼에서 소수 반송자 재결합 수명과 표면 부위 미세 결함에 의한 기계적 손상 평가

최치영, 조상희

경북대학교 무기재료공학과, 대구, 702-701
(1999년 3월 10일 접수)

Abstract We investigated the effect of mechanical back side damage in Czochralski silicon wafer. The intensity of mechanical damage was evaluated by minority carrier recombination lifetime by laser excitation/microwave reflection photoconductance decay (μ-PCD) technique, wet oxidation/preferential etching methods, near surface micro defect (NSMD) analysis, and X-ray section topography. The data indicate that the higher the mechanical damage intensity, the lower the minority carrier lifetime, and NSMD density increased proportionally, also correlated to the oxidation induced stacking fault (OISF) density. Thus, NSMD technique can be used separately from conventional etching method in OISF measurement.

요 약 초크랄스키 실리콘 기판의 뒷면에 형성된 기계적 손상이 미치는 효과에 대하여 고찰하였다. 기계적 손상의 정도는 레이저 여기/극초단파 반사 광전도 감쇠법에 의한 소수반송자 재결합 수명, 습식산화/선택적 식각 방법, 표면 부위 미소 결함 및 X-선 단면 측정 분석으로 평가하였다. 그 결과, 웨이퍼 뒷면에 가해지는 기계적 손상의 세기가 강할수록 소수반송자 재결합 수명은 짧아지고, 표면 부위 미소 결함 밀도는 비례적으로 증가하였으며, 산화 유기 적층 결함 밀도와도 상호 일치하였다. 그래서, 표면 부위 미소 결함 기술은 산화 유기 적층 결함을 측정하는데 있어서 통상적인 부식 방법과는 별도로 사용될 수 있다.

1. Introduction

It has been reported [1, 2] that laser excitation/microwave reflection photoconductance decay (μ-PCD) method is a noncontact, nondestructive, and high throughput technique with higher sensitivity than secondary ion mass spectroscopy and total reflection X-ray fluorescence spectrometry from the metal contamination monitoring point of view. Also it is commonly recognized that minority carrier lifetime measured by the μ-PCD technique is very sensitive to crystallographic defects which can act as trap centers [3]. The other technique is bulk microdefect (BMD) analyzer, and it is applicable to monitoring process-induced defects in the manufacturing processes of very large scale integration (VLSI). An image of the defects is nondestructively obtained by function of laser scattering tomography [4, 5] with the analyzer, then this defect image undergoes binary image processing as in a defect counter, making it possible to obtain a defect density profile. This apparatus features (1) nondestructive observation, (2) three-dimensional observation, (3) measurement of defect density per unit volume, and (4) quantitative determination of denuded zone width. It also makes completely automatic measurement functions possible. Further, by analyzing the scattering intensity per particle, information of defect size can be obtained [6]. Near surface micro defect (NSMD) means small oxidized precipitate of 0~10

μm depth underneath the surface, except bulk microdefect of the wafer bulk generated by repeated heat treatment process during device fabrication.

In silicon wafer industry, the mechanical damage method, which provides dislocation and/or stacking fault nuclei [7, 8] on wafer back side, is one of the extensively used extrinsic gettering techniques [9] since it is simple and inexpensive.

In this work, electrical and structural evaluations on the effect of mechanical damage on back side in Czochralski (CZ) silicon wafers were executed by μ-PCD technique, wet oxidation/preferential etching methods, NSMD measurment, and X-ray section topography.

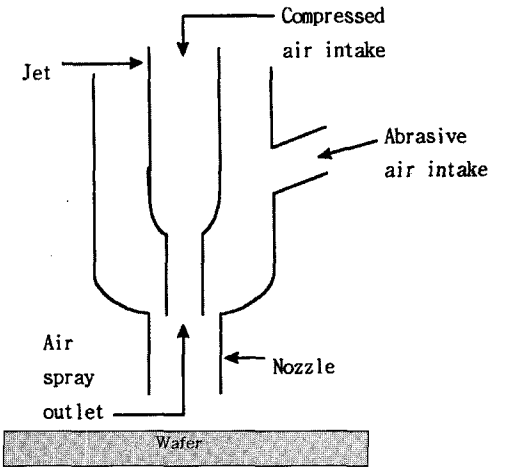

Fig. 1. Schematic of liquid honing method.

2. Experimental

The starting materials in this study were p-type (boron-doped, 9~20 Ω · cm) CZ silicon wafers, with 200 mm diameters (100), single-side polished, and 725 μm thick. The oxygen concentration measured with a Fourier transform infrared (FTIR) spectrometer (Bio-RAD QS-300) according to the New ASTM procedure (ASTM F121-81) [10] was 13.3~16.6 ppma, whereas the carbon level was less than 0.05 ppma which is below the detection limit of FTIR.

The wafers were heat treated at 700℃ for 10 min in N_2 ambient for oxygen donor annihilation [11] and each cleaved into quarter pieces. One piece from each wafer was not mechanically damaged. It was designated as the "reference" to be distinguished from the second, the third and the fourth pieces, and the other three were also designated as grade 1, grade 2, and grade 3, whose back sides were mechanically damaged with three kinds of grades as shown in Table 1, respectively, by using liquid honing method (in Fig. 1).

After the liquid honing process, the samples were cleaned by RCA cleaning method and subjected to surface passivation treatments, such as HF dipping for 10 min by high purity 49 % HF chemical of semiconductor grade and dry oxidation at 1000℃ for 40 min (the thickness of grown oxide layer is about 400 Å), to minimize surface recombination velocity for lifetime measurements [12].

Table 1
Liquid honing process parameters

Grade	Air pressure* (kgf/cm^2)	Conveyer speed* (mm/sec)	No. of nozzle*
1	1	12.3	1
2	4.3	12.3	1
3	5.7	10	2

*: normalized value.

The laser excitation/microwave reflection photoconductance decay (μ-PCD) lifetime measurements for the samples were performed at room temperature using a WT-85X lifetime scanner system (SEMILAB). The silicon wafer was positioned on a wafer mounting stage driven by computer-controlled motors to provide the x-y mapping capability over the wafer surface. A pulsed laser diode with wavelength of 904 nm and 200 ns pulse width was applied for the excitation of the excess carriers. The light source was concentrated at a spot of ~1 mm^2. A microwave system operating at a frequency of 10.3 GHz was used for the detection of the conductivity decay curve from which the time constant (lifetime) of the recombination process could be calculated.

In order to reveal the defects generated as a result of relieving the stresses caused by the liquid honing method, the samples were oxidized at 1100℃ for 60 min in wet oxygen ambient, and then the oxidation induced stacking fault (OISF) was inspected under the optical microscope after Wright etching [13] for 1 min.

The NSMD was also measured by using BMD analysis system (MO-521: Mitsui Mining and Smelting Co, Ltd.) after HF dipping was executed to strip the films oxidized by the same heat treatment. Particularly, MO-521 system was used to measure

the depth underneath the surface; 5×250×500 μm (in depth×width×length). Laser power of 100 mW and 680~700 μm wavelength were exploited, and detection limit was 10 nm φ. We could obtain the number of defects, average scattering intensity, size, area, and volume distribution by this method. We also could measure the samples of grade 1, 2, and 3 on the same conditions, that is, the "Fixed-On" and 10 % of neutral density (ND) filter—parameter of the weakest optic quantity, to estimate the number of defects by relative mechanical damage.

The stresses on as-received wafers caused by mechanical damage were evaluated by employing X-ray section topography system (Bede L6).

3. Results and discussion

3.1. Relationship between mechanical damage intensity and lifetime

Figure 2 (a) shows minority carrier recombination lifetime data measured by μ-PCD technique in nondamaged ("reference") and mechanically damaged back side of silicon wafers. Mechanically damaged sites can provide the nucleation centers for thermally induced dislocations [14] and mechanical damages on a wafer backside can originate slip dislocations which propagate to the front side of the wafer. Moreover, dislocation act effectively as generation-recombination centers and introduce surface states; thus dislocations decrease the minority carrier lifetime [15].

Figure 2 (b) clearly shows that the higher the mechanical damage intensity, the lower the minority carrier lifetime. It is well known that the actual penetration depth of laser beam (904 nm wavelength) into silicon crystal bulk is less than 30 μm [16].

However, as shown in Fig. 2, it is obvious that electrons and holes excited by laser beam are propagated up to wafer back side, consequently affecting the minority carrier recombination lifetime value. That is the reason why a rough estimation for the diffusion length of carriers is about 10 times the penetration depth of laser beam as shown by Tajima *et al.* [17]. Judging from this, we can suggest that nondamaged wafers be used to obtain correct data for contamination and defect monitoring during device processing.

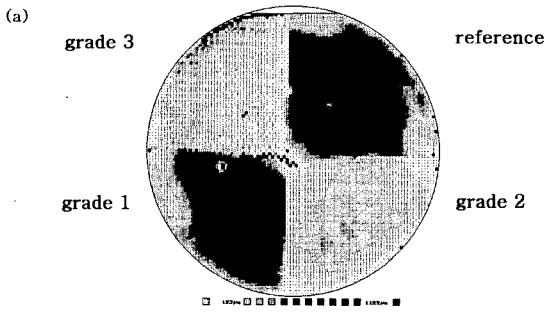

Damage grade	reference	grade 1	grade 2	grade 3
Average lifetime value (μs)	894.4	846	233.1	158.8

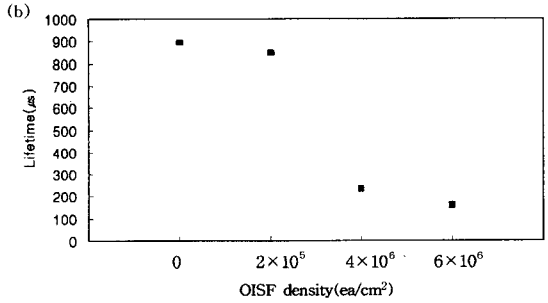

Fig. 2. Relationship between mechanical damage intensity and minority carrier recombination lifetime meaured by μ-PCD technique. (a) lifetime mapping data and average values and (b) trend of average lifetime values.

3.2. Characterization of stresses by mechanical damage

To evaluate the stresses caused by the liquid honing method, we have performed OISF, NSMD, and X-ray section topography analyses. Figures 3 (a)-3 (c) show the defects on the front side of the samples generated during wet oxidation at 1100°C for 60 min as a result of relieving the stresses caused by liquid honing method, and the data as follows; grades 1, 2, and 3 are 2×10^5, 4×10^6, and 6×10^6 ea/cm^2, respectively. In spite of a micronic area of 10×10 μm by atomic force microscope, we can observe that the density of small pit increases according as the mechanical damage intensity does. Thus, the sites at the surface can provide the nucleation centers for OISF, and the OISF density depends primarily on the density of effective nucleation sites.

Note that the harder the mechanical damage intensity, the higher the OISF density. It can be deduced that OISF test method would be a useful way to distinguish mechanical damage grades. The

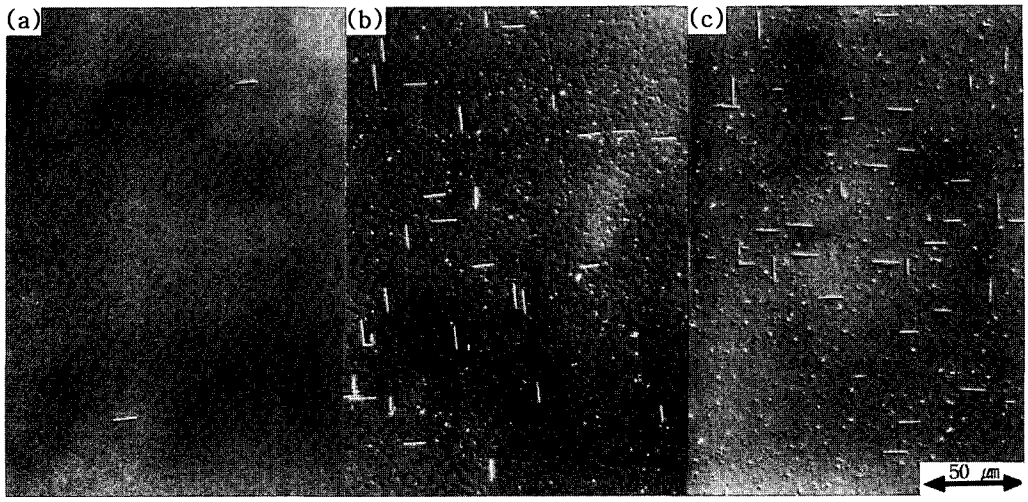

Fig. 3. Oxidation induced stacking faults for the (a) grade 1, (b) grade 2, and (c) grade 3 generated during wet oxidation at 1100°C for 60 min.

BMD analyzer, as the way of evaluation to investigate relative sizes (diameter or volume) of oxygen precipitates, has a function that carries out image processing of defect images obtained by function of laser tomography, determines the location of defects, and then caculates the scattering intensity profile and the defect density profile [6]. Median among the five measuring points of the center area of a sample was chosen as the data. For the image processing, surface particle by P-component scattering and near surface internal defect were measured simultaneously. After that, only genuine internal defect can be acquired by S-component scattering except surface particle. Laser tomograms of each sample were shown in Fig. 4. The difference in NSMD density was clearly distinguishable by showing the higher NSMD density of 4.8×10^6, 2.3×10^8, and 7.2×10^8 ea/cm^3 as the mechanical damage grade goes higher from the grade 1 to grades 2 and 3. On the other hand, NSMD density for the reference wafer is equally zero to the OISF density.

Relationships between NSMD, OISF density and the damage intensity are correlated proportionally. Therefore NSMD techinique, which is different from conventional etching method (OISF test), can be used by another method of defect monitoring.

Since the diffracting X-rays are highly sensitive to lattice strain, this can be exploited in imaging, and defects and wafer quality can be identified by section topography. Figure 5 represents X-ray sec-

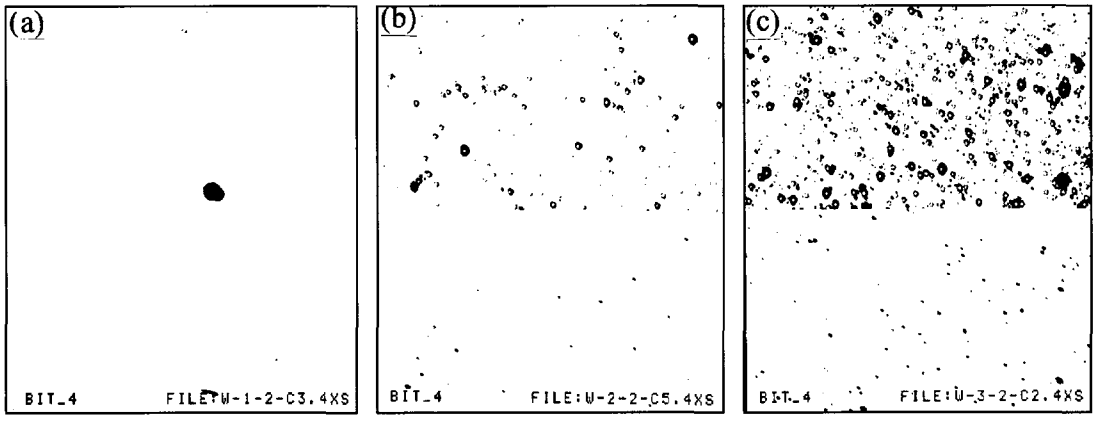

Fig. 4. Laser tomogram of NSMD for the (a) grade 1, (b) grade 2, and (c) grade 3 by image processing.

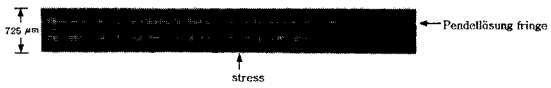

Fig. 5. The stresses revealed by X-ray section topograph. [(440) reflection, Mo $K\alpha_1$].

tion topography of grade 1 sample for (440) reflection with the Mo $K\alpha_1$ radiation. In X-ray topography, image contrast depends on the strain fields of defects, which destroy the coherence of X-ray waves. Pendellösung fringes, which originate from a perfect crystal by its interference of the X-ray beam, are observed in Fig. 5. The bottom edge which corresponds to the mechanically damaged surface shows a great intensification of diffracted intensity from surface damage. Another line image of a dislocation that stretches from the damaged back side to the other surface appears. It is known that the dislocations have a tendency to stay together in close bundles, and they run roughly normal towards the crystal surfaces [18]. Therefore, it is believed that the nucleation of dislocation bundles (shown as stress) might be formed from the damaged surface by the back side mechanical damage. Moreover, the line image approaching the other surface suggests that some of the dislocations spread out deep into the wafer. Consequently, it is quite natural that dislocations affect the mechanical and electrical properties of silicon wafers.

4. Conclusions

The stresses caused by mechanical damage and their effects were evaluated by minority carrier recombination lifetime by laser excitation/microwave reflection photoconductance decay method, wet oxidation/preferential etching methods, BMD analyzer, and X-ray section topography. The results indicate that:

1) The higher the mechanical damage intensity, the lower the minority carrier recombination lifetime.

2) The NSMD density increased proportionally to mechanical damage grade and also correlated to the OISF density.

3) The NSMD technique can be used by another method of OISF measurement.

References

[1] A. Usami, Proc. IEEE 1991 Int. Conference on Microelectronic Test Structures 4 (1991) 1.
[2] A. Buczkowski, Z.J. Radzimski, G.A. Rozgonyi and F. Shimura, J. Appl. Phys. 72 (1992) 2873.
[3] K. Katayama, Y. Kirino, K. Iba and F. Shimura, Jpn. J. Appl. Phys. 30 (1991) L1907.
[4] K. Moriya and T. Ogawa, Jpn. J. Appl. Phys. 22 (1983) L207.
[5] K. Moriya, J. Crystal Growth 94 (1983) 182.
[6] K. Moriya, K. Hirai, K. Kashima and S. Takasu, J. Appl. Phys. 66 (1989) 5267.
[7] M.L. Polignano, G.F. Cerofolini, H. Bender and C. Claeys, J. Appl. Phys. 64 (1988) 869.
[8] F. Shimura, Semiconductor silicon crystal technology, (Academic Press, Inc., San Diego, 1989) p. 350.
[9] S. Hahn, 1989, International Conference on VLSI and CAD, (KITE/IEEE Korea section) 238.
[10] Annual Book of ASTM Standards, F121-81, (American Society for Testing and Materials, Philadelphia, 1987).
[11] V. Cazcarra and P. Zunino, J. Appl. Phys. 51 (1980) 4206.
[12] D.K. Schroder, Semiconductor material and device characterization, (John Wiley & Sons, Inc., New York, 1990) p. 359.
[13] M.W. Jenkins, J. Electrochem. Soc. 124 (1977) 757.
[14] P. Rai-Choudhury and W.J. Takei, J. Appl. Phys. 40 (1969) 4980.
[15] W. Shockley and W.T. Read, Phys. Rev. 87 (1952) 835.
[16] C. Fujihira, M. Morin, H. Hashizume, J. Friedt, Y. Nakai and M. Hirose, Jpn. J. Appl. Phys. 32 (1993) L1362.
[17] M. Tajima, S. Kishino, M. Kanamori and T. Iizuka, J. Appl. Phys. 51 (1980) 2247.
[18] A.R. Lang and A. Authier, Diffraction and Imaging Techniques in Material Science, 2nd ed., edited by S. Amelinckx, R. Gevers and J. Van Landuyt Vol. 2 (North-Holland, Amsterdam, 1978) p. 672.